Monomer−Dimer Equilibrium and Oxygen Binding Properties of Ferrous *Vitreoscilla* Hemoglobin†

Laura Giangiacomo,‡,§ Marco Mattu,‡,|| Alessandro Arcovito,§ Giancarlo Bellenchi,|| Martino Bolognesi,⊥ Paolo Ascenzi,||,⊥ and Alberto Boffi*,§

Dipartimento di Biologia, Università Roma Tre, Viale Guglielmo Marconi 446, I-00146 Roma, Italy, Dipartimento di Scienze Biochimiche A. Rossi Fanelli and CNR-Centro di Biologia Molecolare, Università di Roma La Sapienza, Piazzale Aldo Moro 5, I-00185 Roma, Italy, and INFM-Dipartimento di Fisica e Centro per le Biotecnologie Avanzate, Università di Genova, Largo Rosanna Benzi 10, I-16132 Genova, Italy

Received January 18, 2001; Revised Manuscript Received March 20, 2001

ABSTRACT: The monomer−dimer equilibrium and the oxygen binding properties of ferrous recombinant *Vitreoscilla* hemoglobin (*Vitreoscilla* Hb) have been investigated. Sedimentation equilibrium data indicate that the ferrous deoxygenated and carbonylated derivatives display low values of equilibrium dimerization constants, 6×10^2 and 1×10^2 M^{-1}, respectively, at pH 7.0 and 10 °C. The behavior of the oxygenated species, as measured in sedimentation velocity experiments, is superimposable to that of the carbonylated derivative. The kinetics of O_2 combination, measured by laser photolysis at pH 7.0 and 20 °C, is characterized by a second-order rate constant of 2×10^8 M^{-1} s^{-1} whereas the kinetics of O_2 release at pH 7.0 is biphasic between 10 and 40 °C, becoming essentially monophasic below 10 °C. Values of the first-order rate constants (at 20 °C) and of the activation energies for the fast and slow phases of the *Vitreoscilla* Hb deoxygenation process are 4.2 s^{-1} and 19.2 kcal mol^{-1} and 0.15 s^{-1} and 24.8 kcal mol^{-1}, respectively. Thus the biphasic kinetics of *Vitreoscilla* Hb deoxygenation is unrelated to the association state of the protein. The observed biphasic oxygen release may be accounted for by the presence of two different conformers in thermal equilibrium within the monomer. The two conformers may be assigned to a structure in which the heme−iron-bound ligand is stabilized by direct hydrogen bonding to TyrB10 and a structure in which such interaction is absent. The slow interconversion between the two conformers may reflect a very large conformational rearrangement in the disordered distal pocket segment connecting helices C and E.

Bacterial hemoglobins (Hbs)[1] represent a new frontier in the study of hemoproteins due to their widespread occurrence among diverse species as well as to their multiple and/or still unexplained functions (*1*−*3*). From the structural viewpoint, three different types of bacterial Hbs have been identified: classical eight-helix Hbs, truncated two-over-two α-helical sandwich Hbs, and flavoHbs (*1*, *4*−*7*).

The first bacterial Hb was isolated from the obligate aerobe *Vitreoscilla* sp., a species that uses oxygen as the sole electron acceptor in oxygen-poor environments (*8*−*11*) and has been shown to possess the classical eight-helix Hb fold (*5*, *6*). The functional role of *Vitreoscilla* Hb was initially proposed to be that of myoglobins (Mbs) in that its expression, enhanced in microaerophilic environments, induces a local increase of oxygen concentration that could increase the activity of terminal oxidases (*12*, *13*). Under oxygen-limiting conditions, the increased activity of terminal oxidases is reflected in higher cell density and faster growth when *Vitreoscilla* Hb is coexpressed in heterologous bacteria. Alternatively, *Vitreoscilla* Hb may act itself as a terminal oxidase (*14*). Interestingly, a FAD-containing reductase domain copurifies with *Vitreoscilla* Hb and has been shown to be able to transfer electron(s) to the hemoprotein (*15*). Hence, the noncovalent assembly of *Vitreoscilla* Hb with the FAD-containing reductase domain could yield a flavohemoglobin (flavoHb) whose function may be related to that of single-chain flavoHbs (*4*−*6*, *16*). In this framework, the noncovalent *Vitreoscilla* Hb/FAD-containing reductase domain complex might be involved in NO dioxygenase activity, as recently proposed for genuine flavoHbs (*17*−*22*).

Although all the hypotheses on the functioning of *Vitreoscilla* Hb are related to O_2 reactivity, the only report on the ligand binding properties of the ferrous recombinant bacterial Hb concerns the characterization of the carbon monoxide binding kinetics (*23*), the oxygen binding properties being virtually unexplored.[2] In contrast, cyanide, azide, thiocyanate, and imidazole binding to ferric *Vitreoscilla* Hb has been investigated in detail by both thermodynamic and kinetic viewpoints (*5*). In parallel, the three-dimensional

† This work was supported by grants from the Ministry of University, Scientific Research and Technology of Italy (MURST) and from the National Research Council of Italy (CNR, target oriented project Biotecnologie to P.A.).

* Corresponding author. Tel: +39+06+4940543. Fax: 39+06+4440062. E-mail: alberto.boffi@uniroma1.it.

‡ These authors contributed equally to this work.

§ Università di Roma La Sapienza.

|| Università Roma Tre.

⊥ Università di Genova.

[1] Abbreviations: Hb, hemoglobin; flavoHb, flavohemoglobin; legHb, leghemoglobin; Mb, myoglobin; *Vitreoscilla* Hb, *Vitreoscilla* hemoglobin; DTT, dithiothreitol; PMSF, phenylmethanesulfonyl fluoride.

10.1021/bi0101143 CCC: $20.00
Published on Web 07/07/2001

structures of the ligand-free pentacoordinated ferric *Vitreoscilla* Hb and of its azide, thiocyanate, and imidazole derivatives have been solved at atomic resolution (*5*, *6*).

Inspection of the three-dimensional structures of ferric liganded and unliganded *Vitreoscilla* Hb derivatives shows that the heme distal site is very different from that characteristic of (non)vertebrate Hbs, being filled by residues PheCD1, ProE8, GlnE7, and LeuE11 (*5*, *6*). Interestingly, the polypeptide segment connecting helices C and E is disordered, and residues GlnE7−AlaE10 do not adopt the usual α-helical conformation, thus locating the heme distal residue GlnE7 out of the heme pocket. Azide, imidazole, and thiocyanate binding to the heme iron introduces substantial structural perturbations in the heme distal site residues TyrB10 and ProE8. In particular, residue ProE8 moves away from the heme and triggers the opening of the distal site cavity with the concomitant displacement of the GlnE7−AlaE10 region. Thus, azide, imidazole, and thiocyanate find sufficient room for binding, TyrB10 providing the stabilization of the heme−iron-bound ligand (*5*, *6*). Notably, heme−iron-bound azide and thiocyanate are stabilized by a water molecule bridging the ligand and the TyrB10 residue. By contrast, the phenolic hydroxyl of TyrB10 appears to stabilize the iron-bound imidazole by direct hydrogen bonding.

The quaternary assembly of the ligand-free pentacoordinated ferric *Vitreoscilla* Hb and of its azide, thiocyanate, and imidazole derivatives is unique among the (non)vertebrate globin family (*5*, *6*, *24*, *25*). In fact, *Vitreoscilla* Hb is dimeric within the crystalline lattice and is characterized by a very small intersubunit contact area (about 430 Å^2) built by the F and H helices of opposing subunits. The interface area buried by the two *Vitreoscilla* Hb subunits involves essentially van der Waals contacts between two juxtaposed hydrophobic patches. No salt bridges are present, and all intersubunit hydrogen bonds are actually mediated by interfacial water molecules (*5*, *6*). Comparison of the intersubunit surfaces from a variety of homodimeric Hbs indicates that the interface region differs widely among different species. In turn, the extension of the subunit contact area is generally correlated to the stability of the homodimer in solution. As an example, the homodimeric cooperative Hb from *Scapharca inaequivalvis* displays a large water-excluded surface between the two subunits (about 2000 Å^2) whereas in ferrous deoxygenated *Petromyzon marinus* Hb the subunit interface is definitely smaller (480 Å^2) (*24*, *26*). As a result, *Scapharca* Hb is a stable dimer in solution in both the ligated and unligated state whereas *P. marinus* Hb displays an oxygen-linked monomer−dimer equilibrium such that under physiological conditions the deoxygenated species dimerizes ($K_{1,2}$ is about 1×10^4 M^{-1}) and the liganded species is monomeric (*26*).

The present study reports the monomer−dimer equilibrium and the oxygen binding properties of ferrous *Vitreoscilla* Hb in order to establish whether the association−dissociation equilibrium is an oxygen-linked process. These results have been analyzed in the light of the available three-dimensional structures of the ferric derivatives (*5*, *6*) and in parallel with those of related oligomeric Hb systems.

MATERIALS AND METHODS

Vitreoscilla Hb Expression and Purification. Recombinant *Vitreoscilla* Hb was expressed in *Escherichia coli* as previously reported (*6*). However, purification of recombinant ferric *Vitreoscilla* Hb was carried out with a new procedure in which ammonium sulfate precipitation was avoided. In fact, extensive heme loss, low protein recovery, and Cys oxidation (i.e., loss of titrability by *p*-chloromercuribenzoate) were observed after precipitation with 40%, accurately buffered (pH = 7.0) ammonium sulfate.

After sonication, the crude bacterial extract (suspended in 2.5×10^{-2} M Tris-HCl buffer, pH 7.5, 1.0×10^{-3} M EDTA, 2.0×10^{-3} M DTT, and 1.0×10^{-4} M PMSF) was loaded directly onto a DEAE-52 cellulose column and eluted with a NaCl gradient from 2.5×10^{-2} to 4.0×10^{-1} M. The reddish fraction eluted at 1.5×10^{-1} M NaCl. Fractions with an absorbance ratio 416/280 nm higher than 1 were pooled, dialyzed against bidistilled water containing 1.0×10^{-3} M EDTA and 1.0×10^{-3} M DTT (pH was adjusted to 7.5 by addition of sodium bicarbonate), and loaded on a Microceramic hydroxylapatite column (Bio-Rad) equilibrated with the same solution. A sodium phosphate gradient (from 0 to 5.0×10^{-2} M, pH 7.0) was applied and the protein eluted at a buffer concentration of about 1.5×10^{-2} M. Fractions with an absorbance ratio 416/280 nm higher than 2 were pooled, loaded on a MonoQ FPLC column (Pharmacia), and eluted with a NaCl gradient from 5.0×10^{-2} to 1.5×10^{-1} M. Ferrous *Vitreoscilla* Hb was higher than 98% pure as judged by gel electrophoresis, performed under denaturing and nondenaturing conditions, N-terminal amino acid sequence determination, and mass spectroscopy. All purification steps were carried out at 4 °C.

Sedimentation Equilibria of Vitreoscilla Hb. Sedimentation equilibria were performed on the deoxygenated and carbonylated derivatives of ferrous *Vitreoscilla* Hb at pH 7.0 (1.0×10^{-1} M phosphate buffer containing 2.0×10^{-2} M sodium dithionite) and 4.0 and 10.0 °C. Ultracentrifuge runs were performed at 30 000 or 40 000 rpm using a Beckman XL-A analytical ultracentrifuge equipped with absorbance optics and an An60-Ti rotor. Data were collected at a spacing of 1.0×10^{-3} cm with 10 averages in a step scan mode every 3 h. Equilibrium conditions were checked by comparing scans up to 24 h. Data sets were fitted with NONLIN (PC version provided by E. Braswell, National Analytical Ultracentrifugation Center, Storrs, CT). *Vitreoscilla* Hb concentration varied between 3.5×10^{-6} and 1.6×10^{-4} M. As a control of the state of ligation, the absorbance spectra of all protein samples were measured in the ultracentrifuge cells before and after each run. For fitting to the monomer−dimer equilibrium, the molecular mass of monomeric *Vitreoscilla* Hb was fixed to the value obtained from the amino acid sequence (15 775 kDa; *27*). The oxygenated derivative of *Vitreoscilla* Hb was observed to autoxidize even at 4.0 °C, during the time needed to perform the sedimentation equilibrium measurement (48−56 h). Thus, sedimentation velocity experiments were carried out on the oxygenated *Vit-*

[2] To clear up ambiguities, it must be pointed out that recombinant *Vitreoscilla* Hb is a different protein with respect to the so-called "cytochrome *o*", a soluble hemoprotein obtained from *Vitreoscilla* species. In particular, the molecular mass of the monomeric species (13 000 Da in cytochrome *o* versus 17 000 Da in *Vitreoscilla* Hb) and the amino acid composition differ (*8*−*11*, *26*). Thus, we feel that comparison with literature data referring to cytochrome *o* (*8*−*11*) must take these differences into account.

reoscilla Hb derivative in parallel with either the deoxygenated or carbonylated species. In these experiments, data were collected at 40 000 rpm, the monochromator was set at 412 or 540 nm, depending on protein concentration (from 1.0×10^{-5} to 2.0×10^{-4} M). Free cysteine titrability was checked by PMB titrations at the end of the ultracentrifuge runs after removal of DTT or dithionite by gel filtration on a G-25 column. The control of the oxidation state of the sulfydryl groups is essential in order to establish that the association state is not dependent on a disulfide-linked dimer. In fact, previous purification procedures carried out in the absence of DTT resulted in the formation of variable amounts of disulfide-linked dimers, which however were promptly reversed by dialyzing the protein in the presence of 0.5−1 mM DTT.

Oxygen Binding to Vitreoscilla Hb. The oxygenation kinetics of ferrous *Vitreoscilla* Hb were measured at pH 7.0 (1.0×10^{-1} M phosphate buffer) in the presence of 1.0×10^{-3} M EDTA and 1.0×10^{-3} M DTT and at 20.0 °C by laser photolysis. The measurements have been carried out using as an optical pump the second harmonic from a Quanta System Nd:YAG laser ($\lambda = 532$ nm, frequency of 2 Hz with a pulse width of 5 ns and pulse energy of approximately 80 mJ). This laser pulse flashes the sample in a tonometer with a quartz cell of 1 cm length orthogonally to the optical probe due to a small intensity (25 W) UV−visible source focused onto a monochromator SPEX 1681. Single-wavelength measurements have been acquired using as detector a Hamamatsu R1398 photomultiplier tube. The time courses have been averaged and recorded using a Tektronix TDS 360 digital oscilloscope. The time courses (average of 50 traces) of *Vitreoscilla* Hb oxygenation were followed at 412 and 432 nm as a function of O_2 concentration (ranging between 2.2×10^{-5} and 1.4×10^{-3} M) at a protein concentration of 1.1×10^{-5} M.

Oxygen dissociation kinetics were obtained by mixing oxygenated *Vitreoscilla* Hb in the presence of 1.0×10^{-3} M EDTA and 1.0×10^{-3} M DTT with sodium dithionite solutions (2.0×10^{-2} to 1.0×10^{-1} M). Observation wavelengths were 416 and 434 nm. Experiments were carried out with an Applied Photophysics rapid-mixing stopped-flow apparatus (Leatherhead) between pH 6.0 and 9.0 and between 5.0 and 40.0 °C. *Vitreoscilla* Hb concentration ranged between 2.0×10^{-5} and 4.0×10^{-5} M. Absorption spectra as a function of time (time resolution 0.125 s) were also measured in the same stopped-flow apparatus, at pH 7.0 and 20.0 °C, by means of a diode array device. The following buffer systems (all 2.5×10^{-1} M) were used: Bis-Tris-HCl (pH 6.0), phosphate (pH 7.0), and Tris-/HCl (pH 8.0 and 8.7).

RESULTS

Sedimentation Equilibria of Vitreoscilla Hb. Sedimentation equilibria of deoxygenated and carbonylated *Vitreoscilla* Hb are shown in Figure 1. The data analysis (see Materials and Methods) allowed the determination of the monomer−dimer equilibrium association constant ($K_{1,2}$) values [$(6 \pm 1) \times 10^2$ M^{-1} and $(1 \pm 0.6) \times 10^2$ M^{-1} for the deoxygenated and carbonylated derivatives, respectively], at pH 7.0 and 10 °C. A slight increase in the values of $K_{1,2}$ was observed at 4 °C (about 9×10^2 M^{-1} and 2.5×10^2 M^{-1} for the deoxygenated and carbonylated derivatives, respectively).

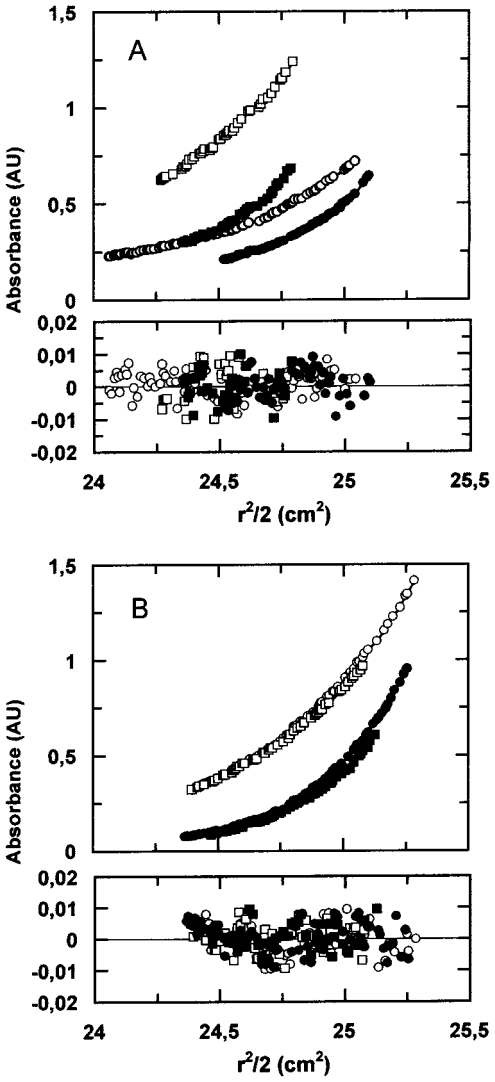

FIGURE 1: Sedimentation equilibria of deoxygenated (panel A) and carbonylated (panel B) *Vitreoscilla* Hb. Data were obtained at 30 000 (○, □) and 40 000 (●, ■) rpm at protein concentrations of 3.5×10^{-5} M (○, ●) and 1×10^{-4} M (□, ■) in 0.1 M phospate buffer at pH 7.0 containing 1×10^{-3} M EDTA and 1×10^{-3} M DTT at 10 °C. The analysis of the data in terms of monomer−dimer equilibrium yielded values of $K_{1,2}$ of $6 \pm 1 \times 10^2$ M^{-1} and $1 \pm 0.4 \times 10^2$ M^{-1} for the deoxygenated and carbonylated derivatives, respectively. The error distributions are also shown.

The association state of the oxygenated derivative of *Vitreoscilla* Hb could not be measured in equilibrium experiments due to the relatively fast autoxidation rate ($t_{1/2}$ of about 16 h), even in the presence of 1.0×10^{-3} M DTT. Therefore, sedimentation velocity measurements were performed on the oxygenated derivative of *Vitreoscilla* Hb, the ferric Hb species being less than 10% at the end of the run. The $s_{20,w}$ value for the oxygenated and carbonylated derivatives of *Vitreoscilla* Hb corresponded to 1.7 ± 0.2 at pH 7.0 and between 10 and 20 °C, indicating that both ligated ferrous Hb derivatives are monomeric.

Oxygen Binding Properties of Vitreoscilla Hb. Vitreoscilla Hb oxygenation kinetics are shown in Figure 2. O_2 rebinding after photolysis was characterized by a second-order process, the value of k_{on} being $(2.0 \pm 0.3) \times 10^8$ M^{-1} s^{-1}. The observed rate constant and the relative amplitude of the oxygenation process were independent of protein concentration in the range 4.0×10^{-6} and 1.0×10^{-4} M, under

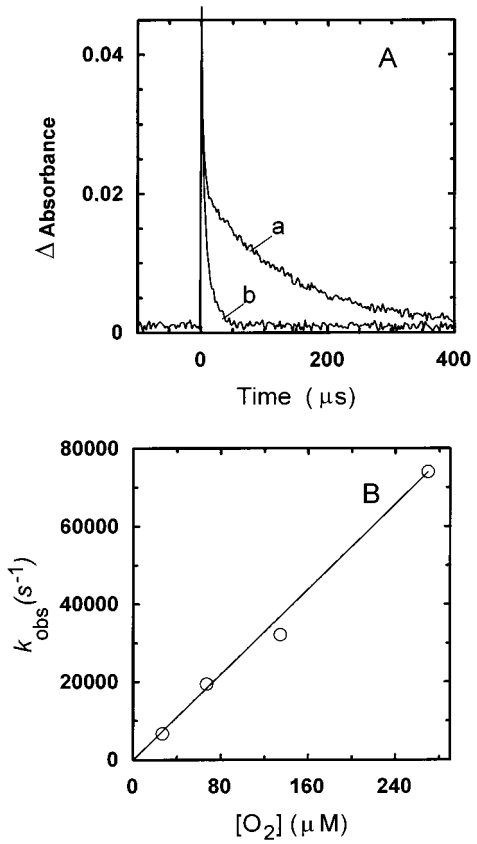

FIGURE 2: Oxygen combination kinetics of *Vitreoscilla* Hb. Oxygen recombination time courses after 9 ns laser photolysis (panel A). The time courses were followed at 412 nm at $[O_2] = 2.2 \times 10^{-5}$ M (trace a) and 2.7×10^{-4} M (trace b). Protein concentration was 6.7×10^{-6} M. Experiments were carried out in 0.1 M phosphate buffer at pH 7.0 and 20 °C. Pseudo-first-order plot for oxygen combination kinetics (panel B). The observed rates (k_{obs}) were obtained by fitting the kinetic records to double exponentials; the fast phase was independent of oxygen concentration and is not reported. Thus, the values of k_{obs} refer only to the O_2-dependent slow phases.

conditions where $[O_2]$ ($=1.0 \times 10^{-3}$ M) > [Hb] (data not shown). Under all experimental conditions, the amount of photolysis was very small, i.e., about 3%, with respect to control experiments carried out on human adult Hb that typically yielded at least 10% of photolysis. In the fastest kinetic records (1 μs time scale), an early relaxation process was observed, ending within 2−3 μs. This fast component was independent of O_2 concentration, possibly reflecting geminate rebinding.

The time course of oxygen dissociation from *Vitreoscilla* Hb, as measured by rapid-mixing stopped-flow experiments, was biphasic and pH independent between pH 6.0 and 8.7 at 20 °C (see Figure 3, panel A). Values of the observed oxygen dissociation rate constants for the fast and slow phases (4.2 ± 0.2 s^{-1} and 0.15 ± 0.04 s^{-1}, respectively, at pH 7.0 and 20 °C) were independent of the observation wavelength between 350 and 470 nm. Both the rate constant and the relative amplitude of the two phases were independent of protein concentration between 4×10^{-6} and 2×10^{-4} M. Both processes reflect oxygen release from *Vitreoscilla* Hb as indicated by the time dependence of the absorption difference spectrum (oxygenated Hb minus deoxygenated Hb). In fact, the difference spectra referring to both fast and slow phases are typical of Hb and Mb deoxygenation processes. Notably, only two spectroscopically distinct species were detected (i.e., oxygenated and deoxygenated *Vitreoscilla* Hb) (Figure 3, panel B).

The observed rate constants and the relative amplitudes of the fast and slow oxygen dissociation phases were found to be strongly dependent on temperature (see Figure 4). In fact, the kinetics of O_2 release from *Vitreoscilla* Hb was biphasic between 10 and 40 °C, becoming essentially monophasic below 10 °C. In particular, the amplitude of the fast phase decreased upon a decrease in temperature, whereas the opposite was observed for the slow component (see Figure 4, panel A). The analysis of data in terms of the Arrhenius equation allowed the estimate of the activation energy values for the fast and slow processes (see Figure 4, panel B). The fast phase of the *Vitreoscilla* Hb deoxygenation process displayed an E_a value of 19.2 ± 0.4 kcal/mol, typical of the activation energy for oxygen dissociation from (non)vertebrate Mbs and Hbs (*27*, *28*). By contrast, the slow phase was characterized by an unusually high E_a value (24.8 ± 1.2 kcal/mol).

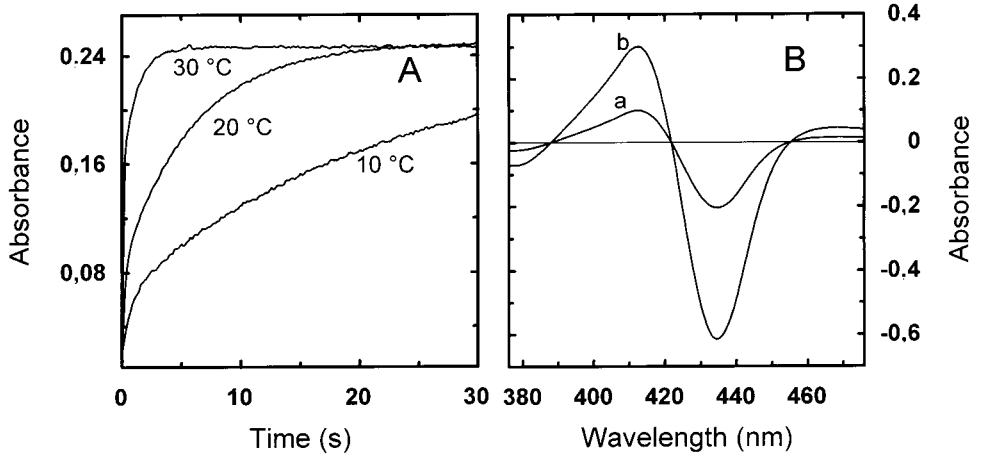

FIGURE 3: Oxygen dissociation kinetics from *Vitreoscilla* Hb. Time courses at three different temperatures are reported in panel A. The observation wavelength was 434 nm. Experiments were performed in phosphate buffer at pH 7.0 (0.25 M) at a protein concentration of 6×10^{-6} M. The difference spectra oxygenated *minus* deoxygenated *Vitreoscilla* Hb are reported in panel B. The spectra were obtained from a diode array experiment, and the amplitude relative to the fast (a) and the slow (b) phases is reported. The experiment was carried out at 20 °C in phosphate buffer at pH 7.0 (0.25 M) at a protein concentration of 1.1×10^{-5} M.

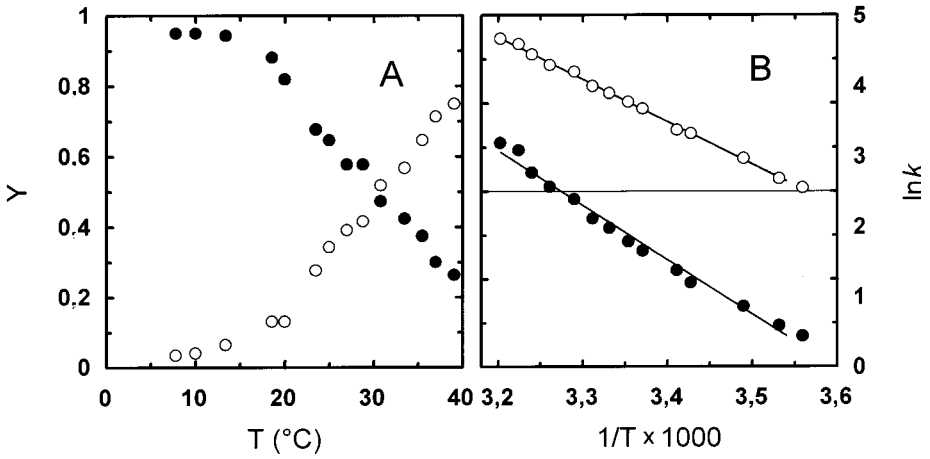

FIGURE 4: Temperature dependence of the oxygen dissociation kinetics in *Vitreoscilla* Hb. The normalized amplitudes (*Y*) of the fast (○) and slow (●) phases are reported as a function of temperature (panel A). The Arrhenius plot relative to the fast (○) and the slow (●) phases of oxygen release kinetics is reported in panel B. The linear fits yielded activation energy values of 19.2 ± 0.4 kcal/mol and 24.8 ± 1.2 kcal/mol for the fast and slow phases, respectively. All data were obtained in phosphate buffer at pH 7.0 (0.25 M).

DISCUSSION

The main target of the present investigation is the charcterization of the oxygen binding properties and of the association state of liganded and unliganded ferrous *Vitreoscilla* Hb derivatives in order to establish whether subunit association is oxygen-linked. The data obtained from sedimentation equilibrium measurements yielded values of $K_{1,2}$ for the deoxygenated and carbonylated derivatives of *Vitreoscilla* Hb of 6×10^2 M^{-1} and 1×10^2 M^{-1}, respectively, at 10 °C and pH 7.0. The association states of the oxygenated *Vitreoscilla* Hb derivative and of the carbonylated species are superimposable, as observed in sedimentation velocity experiments. Although the slight difference between the values of $K_{1,2}$ in the ferrous ligated and unligated *Vitreoscilla* Hb derivatives may suggest ligand-linked association−dissociation phenomena, the monomer−dimer equilibrium is strongly shifted toward the monomeric species in both ligated and unligated derivatives under the experimental conditions here considered. Thus, the ligand-linked dissociation process is not expected to have functional relevance in vivo. In fact, although no quantitative data are available for the *Vitreoscilla* Hb expression levels in *Vitreoscilla* sp., recombinant *Vitreoscilla* Hb concentration in vivo (in *E. coli*) does not exceed 10^{-4}−10^{-3} M at the highest expression levels (*29*). Hence it can be postulated that *Vitreoscilla* Hb is predominantly a monomer under in vivo conditions.

The existence of ferrous *Vitreoscilla* Hb in the monomeric state is consistent with the properties of the subunit interface observed in the crystal structures of ferric derivatives that is characterized by a small intersubunit contact area (430 Å^2) and appears to be stabilized essentially by pairing two hydrophobic patches in the opposing subunits (*5*, *6*).

Oxygen binding properties of *Vitreoscilla* Hb have been investigated over a protein concentration range in which dimer formation does not occur in both the oxygenated and deoxygenated states, on the basis of the ultracentrifugation data. *Vitreoscilla* Hb oxygenation kinetics is characterized by a simple second-order process, with a rate of 2×10^8 M^{-1} s^{-1}, at pH 7.0 and 20 °C. On the other hand, oxygen dissociation kinetics from *Vitreoscilla* Hb is unexpectedly complex for a monomeric hemoprotein. Notably, deoxygenation kinetics was monophasic below 10 °C and biphasic between 10 and 40 °C. At pH 7.0 and 20 °C, values of k_{off} for the fast and the slow phases of the deoxygenation process were 4.2 s^{-1} and 0.15 s^{-1}, respectively.

The simplest way to rationalize the complex kinetic behavior (i.e., the biphasic deoxygenation kinetics) of a monomeric macromolecule containing a single active site is to consider the existence of two conformers in thermal equilibrium. This hypothesis is supported by the temperature dependence of the oxygen release process in *Vireoscilla* Hb, as indicated by the Arrhenius plot of Figure 4. Interestingly, the activation energy (E_a) for oxygen release relative to the fast phase (19.2 kcal/mol) is similar to that observed in vertebrate Mbs and Hbs (*27*, *28*) while that relative to the slow process is about 6 kcal/mol higher. The major contribution to E_a in a simple monomolecular oxygen dissociation process comes from the intrinsic stability of the iron−ligand bond, i.e., is directly proportional to the $\Delta H°$ (standard enthalpy of bond formation) value. Thus, the two widely different values of E_a for oxygen release in *Vitreoscilla* Hb may reflect two different stabilization modes of the heme−iron-bound ligand. Accordingly, the slow O_2 dissociating conformer may receive a strong stabilizing contribution (i.e., hydrogen bonding) from an amino acid distal pocket residue (namely, TyrB10) whereas in the fast O_2 dissociating conformer this interaction is not present or may be mediated by a bridging water molecule. Interestingly, the heme−iron-bound azide and thiocyanate are stabilized by a water molecule bridging the ligand and the TyrB10 residue. By contrast, direct TyrB10 hydrogen bonding to the iron-bound imidazole has been observed. The presence of two conformers in *Vitreoscilla* Hb is in line with recent findings by Gardner et al. (*20*) and Mukai et al. (*22*) on *E. coli* flavoHb. Gardner et al. observed a kinetic heterogeneity in CO binding to flavoHb whereas Mukai et al. observed two conformers in carbonylated flavoHb on the basis of the appearance of two different CO stretching peaks in the resonance Raman spectrum. The two conformers have been assigned to a "closed" structure in which the iron-bound CO is stabilized by hydrogen bonding to TyrB10 and an "open" conformer

[3] Under vacuum, *Vitreoscilla* Hb does not release O_2 (M. Coletta, personal communication).

in which such interaction is absent (*22*). It should be mentioned that the presence of two conformers has been demonstrated also in the carbonylated derivatives of *Ascaris suum* Hb and *Lucina pectinata* HbII, which share the TyrB10−GlnE7 pair with *Vitreoscilla* Hb (*30*, *31*).

A prerequisite for the observed biexponential kinetics in *Vitreoscilla* Hb is that the two conformers do not interconvert within the time scale of the oxygen release process. At present, it can be inferred that the slowly interconverting conformers are separated by an energy barrier that is much higher than simple rotameric rearrangements. It is tempting to speculate that such slow interconversion is related to local restructuring (with opening) of the distal pocket, which in the crystal structure includes a disordered amino acid segment (the first part of the E helix, up to residue GluE6) and the conformationally restricted ProE8 residue.

Last, it is of interest to discuss the present oxygen binding data in the light of the possible physiological role of *Vitreoscilla* Hb. The oxygen affinity of *Vitreoscilla* Hb, as estimated by the values of kinetic parameters, yields an average affinity constant for oxygen binding at 20 °C in the nanomolar range.[3] This estimate, coupled to the relatively slow rate of oxygen release, indicates that *Vitreoscilla* Hb is not likely to be involved in oxygen transport or storage. These functions in fact require a prompt release of oxygen stimulated by metabolic needs under low oxygen partial pressure (O_2 in the micromolar range) that contrasts with the measured kinetic and estimated thermodynamic parameters in *Vitreoscilla* Hb. At present, the only plausible function of *Vitreoscilla* Hb and other bacterial Hbs may be related to oxygen activation for an oxygenase-like function (*7*, *22*). On this basis, the NO dioxygenase activity shown in *E. coli* flavoHb may occur also in *Vitreoscilla* Hb, through the cooperating action of an efficient electron donor protein.

ACKNOWLEDGMENT

Authors thank Prof. Emilia Chiancone, Prof. Massimo Coletta, and Prof. Maurizio Brunori for helpful discussions.

REFERENCES

1. Bolognesi, M., Bordo, D., Rizzi, M., Tarricone, A., and Ascenzi, P. (1997) *Prog. Biophys. Mol. Biol. 68*, 29−68.
2. Hardison, R. (1998) *J. Exp. Biol. 201*, 1099−1117.
3. Imai, K. (1999) *Nature 401*, 437.
4. Ermler, U., Siddiqui, R. A., Cramm, R., and Friedrich, B. (1995) *EMBO J. 14*, 6067−6077.
5. Bolognesi, M., Boffi, A., Coletta, M., Mozzarelli, A., Pesce, A., Tarricone, C., and Ascenzi, P. (1999) *J. Mol. Biol. 291*, 637−650.
6. Tarricone, C., Galizzi, A., Coda, A., Ascenzi, P., and Bolognesi, M. (1997) *Structure 5*, 487−507.
7. Pesce, A., Couture, M., Dewilde, S., Guertin, M., Yamauchi, K., Ascenzi, P., Moens, L., and Bolognesi, M. (2000) *EMBO J. 19*, 2424−2434.
8. Liu, C. Y., and Webster, D. A. (1974) *J. Biol. Chem. 249*, 4261−4266.
9. Webster, D. A., and Orii, Y. (1977) *J. Biol. Chem. 252*, 1834−1836.
10. Orii, Y., and Webster, D. A. (1986) *J. Biol. Chem. 261*, 3544−3547.
11. Tyree, B., and Webster, D. A. (1978) *J. Biol. Chem. 261*, 3544−3547.
12. Tsai, P. S., Hatzimamikatis, V., and Bailey, J. E. (1995) *Biotechnol. Bioeng. 49*, 139−150.
13. Tsai, P. S., Nagely, M., and Bailey, J. E. (1995) *Biotechnol. Bioeng. 49*, 151−160.
14. Dikshit, R. P., Dikshit, K. L., Liu, Y., and Webster, D. A. (1992) *Arch. Biochem. Biophys. 293*, 241−245.
15. Jacob, W., Webster, D. A., and Kroneck, P. M. (1992) *Arch. Biochem. Biophys. 292*, 29−33.
16. Membrillo-Hernandez, J., Coopmah, M. D., Anjum, M. F., Stevanin, T. M., Kelly, A., Hughes, M. N., and Poole, R. K. (1999) *J. Biol. Chem. 274*, 748−754.
17. Hausladen, A., Gow, A. J., and Stamler, J. S. (1998) *Proc. Natl. Acad. Sci. U.S.A. 95*, 14100−14105.
18.
19. Gardner, P. R., Gardner, A. M., Martin, L. A., and Salzman, A. L. (1998) *Proc. Natl. Acad. Sci. U.S.A. 95*, 10378−10383.
20. Gardner, A. M., Martin, L. A., Gardner, P. R., Dou, Y., Li, T., Olson, J. S., Zhu, H., and Riggs, A. F. (2000) *J. Biol. Chem. 275*, 31581−31587.
21. Gardner, A. M., Martin, L. A., Gardner, P. R., Dou, Y., and Olson, J. S. (2000) *J. Biol. Chem. 275*, 12581−12589.
22. Mukai, M., Mills, C. E., Poole, R. K., and Yeh, S. R. (2000) *J. Biol. Chem.* (in press).
23. Dikshit, K. L., Orii, Y., Navani, N., Patel, S., Huang, H. Y., Stark, B. C., and Webster, D. A. (1998) *Arch. Biochem. Biophys. 349*, 161−166.
24. Heaslet, H. A., and Royer, W. E., Jr. (1999) *Struct. Fold. Des. 7*, 517−526.
25. Royer, W. E., Jr., Hendrickson, W. A., and Chiancone, E. (1990) *Science 249*, 518−521.
26. Qiu, Y., Maillet, D. H., Knapp, J., Olson, J. S., and Riggs, A. F. (2000) *J. Biol. Chem. 274*, 748−754.
27. Antonini, E., and Brunori, M. (1971) *Hemoglobin and Myoglobin in their Reaction with Ligands*, p 223, North-Holland Publishing Co., Amsterdam.
28. Coletta, M., Ascenzi, P., Polizio, F., Smulevich, G., del Gaudio, R., Piscopo, M., and Geraci, G. (1998) *Biochemistry 37*, 2873−2878.
29. Khosla, C., and Bailey, J. E. (1989) *J. Mol. Biol. 210*, 79−89.
30. Peterson, E. S., Huang, S., Wang, J., Miller, L. M., Vidugiris, G., Kloek, A., Goldberg, D. E., Chance, M. R., Wittenberg, J. B., and Friedman, J. M. (1997) *Biochemistry 36*, 13110−13121.
31. Das, T. K., Friedman, J. M., Kloek, A. P., Goldberg, D. E., and Rousseau, D. L. (2000) *Biochemistry 39*, 837−842.

BI0101143